Supporting Information

Rapid Wafer-Scale Growth of Polycrystalline 2H-MoS_2 by Pulsed Metalorganic Chemical Vapor Deposition

Berc Kalanyan[†], *William A. Kimes*[†], *Ryan Beams*[†], *Stephan J. Stranick*[†], *Elias Garratt*[†], *Irina Kalish*[†], *Albert V. Davydov*[†], *Ravindra K. Kanjolia*[‡], *James E. Maslar*[†]

[†]Materials Measurement Laboratory, National Institute of Standards and Technology, Gaithersburg, Maryland 20899, United States;

[‡]EMD Performance Materials, Haverhill, Massachusetts 01835, United States.

Growth Temperature

Growth temperature is expected to be the strongest parameter affecting film quality. To study the influence of process temperature on film crystallinity, we compared XRD patterns obtained from films grown at temperatures ranging from 351 °C to 591 °C. Growth at 351 °C resulted in films that were <8 nm thick (inferred from presence of Si 2p transitions in XPS spectra), which is too thin for conventional XRD analysis. Films grown at ≥400 °C were thick enough to exhibit new reflections in addition to those associated with the substrate. It is evident from Figure S1 that degree of film's crystallinity is dependent on the growth temperature as the full width at half maximum (FWHM) of the (000*l*) family of peaks decreases and d-spacing (c-lattice parameter) decreases with temperature, approaching the values reported in the literature. As expected, the higher index (000*l*) peaks exhibit a larger degree of broadening. Note that growth rate also increases with temperature.

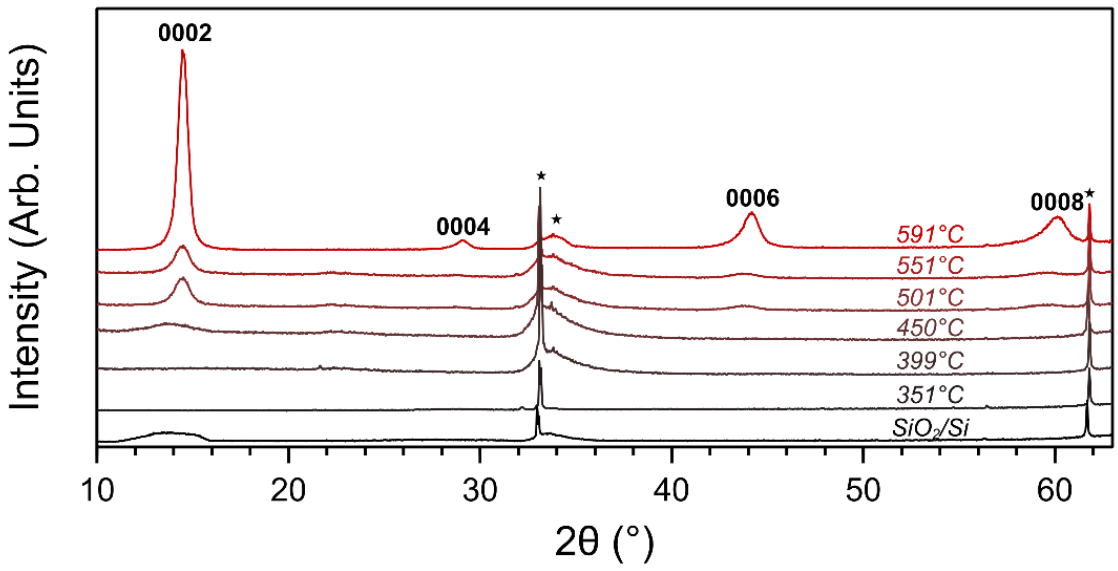

Figure S1. XRD of films (*n*=200) grown at various substrate temperatures. Reflections identified with a star (★) denote substrate peaks.

Peak positions and assignments for the XRD measurements are listed in the following table:

Table S1. Positions and assignments for MoS_2 peaks from XRD measurement on a film grown with *n*=200 at 591 °C.

2θ (°)	**Assignment**
14.46	MoS_2 (0002)
29.06	MoS_2 (0004)
44.18	MoS_2 (0006)
60.140	MoS_2 (0008)

Onset of Film Nucleation

High resolution XPS spectra that capture the early nucleation of MOCVD films are shown in Figure S2. The Mo 3d region for a film grown with one injection of precursors (*n*=1)

clearly shows a Mo 3d doublet assigned to oxidized Mo. The signal to noise ratio is not high enough to discern any additional peaks. After three injections (n=3), a lower binding energy doublet assigned to MoS_2 emerges, alongside the corresponding S 2s peak. The presence of Mo on the surface even after one injection indicates that the incubation time on the SiO_2 surface is negligible for our MOCVD process under the conditions examined.

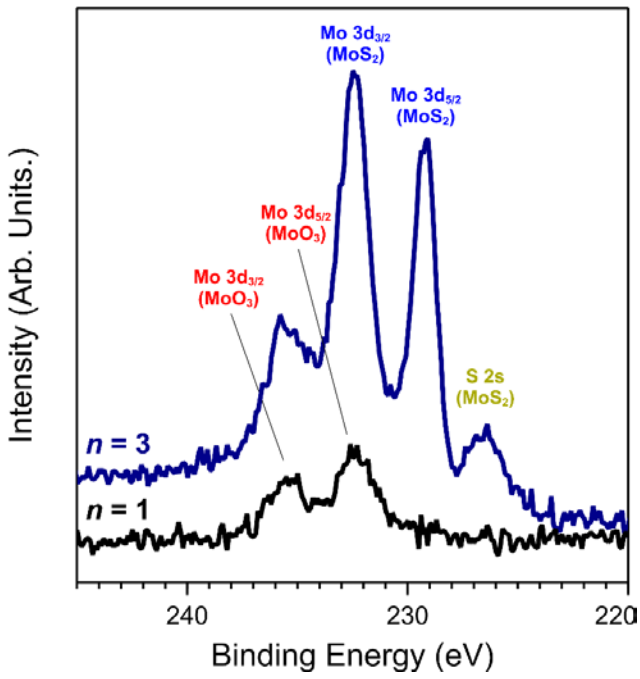

Figure S2. High resolution XPS spectra from films grown using n=1 and n=3 showing the early onset of Mo 3d and S 2s peaks.

Film Topography and Roughness

Topographic AFM maps of the MOCVD grown films are presented in Figure S3 for the full set of film thicknesses (n=1 to n=200) explored in this study. Measurements for n=50 and n=100 show distinct tall features that correspond with surface roughness also observed in SEM images in Figure 4 and Figure S4.

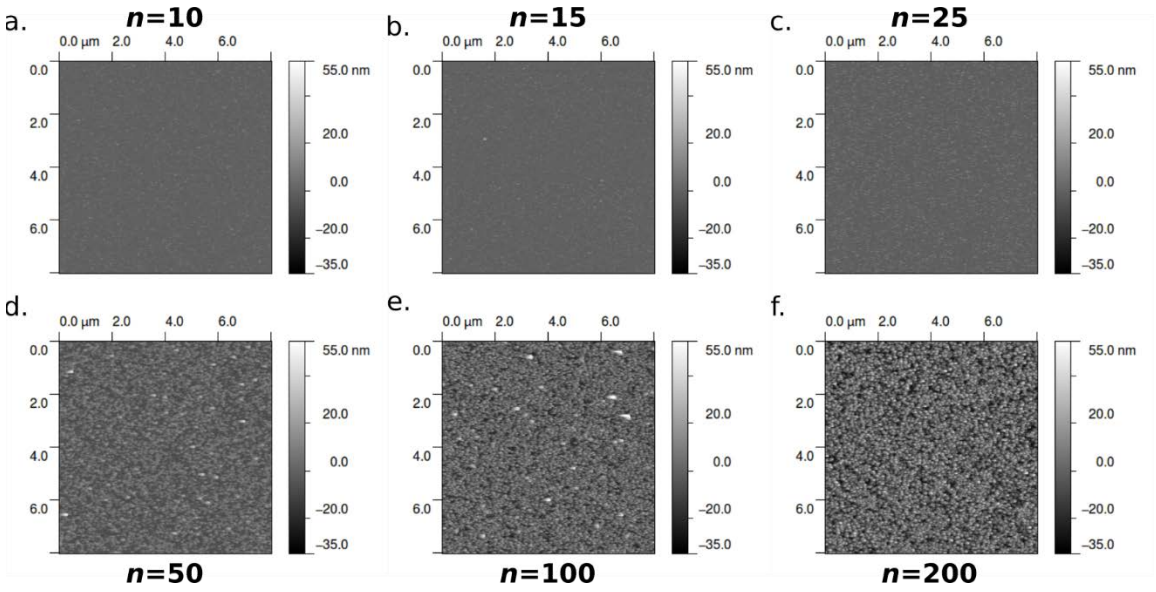

Figure S3. AFM topographic scans for (a) n=10, (b) 15, (c) 25, (d) 50, (e) 100, and (f) 200.

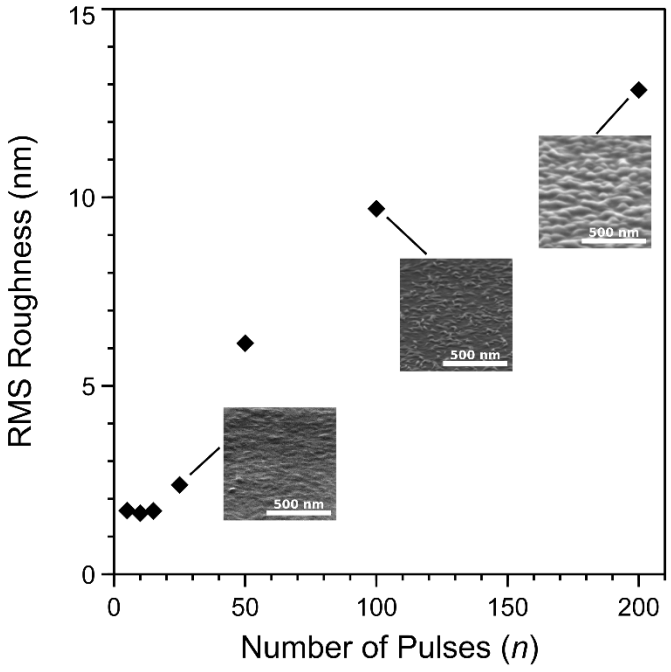

Figure S4. RMS roughness vs n, with accompanying SEM images

Thickness Determination from XPS

Thickness estimation using XPS relies on the calculation of an inelastic mean free path (IMFP) value (λ) for Si 2p photoelectrons originating within the SiO_2/Si substrate. The IMFP estimate based on the TPP-2M method[1] is implicitly dependent upon the composition of the thin film overlayer, since λ is a function of density, valence electron count, and band gap. Given that our MOCVD films contain carbon residue and a MoO_3 native oxide, we considered the sensitivity of λ to film composition. The thickness of the native oxide is expected to have a negligible contribution to the thickness calculation, since Si 2p attenuation from MoS_2 and MoO_3 overlayers are nearly equivalent, with $\lambda_{MoO_3} = 2.512$ and $\lambda_{MoS_2} = 2.465\ nm$. Carbon, however, is about 1.3 times less attenuating than either MoS_2 or MoO_3 (λ_{carbon}=3.364 nm for 1383 eV electrons). Therefore, depending on fractional carbon content, our thickness estimate from Si 2p attenuation may underreport MoS_2 thickness by approximately 30%. Regardless of the absolute IMFP value used in this analysis, the trends observed in the thickness estimate (Figure 4 in the main text) are valid.

Overlayer thickness was calculated using the following expression[2]:

$$t_{MoS_2} = -\lambda_{MoS_2} \ln\left(A_{Si\ 2p}/A_{Si\ 2p,0}\right)$$

Where t_{MoS_2} is the overlayer thickness in nm, λ_{MoS_2} is the IMFP for the overlayer, $A_{Si\ 2p,0}$ is the initial Si 2p peak area for a bare substrate, and $A_{Si\ 2p}$ is the Si 2p peak area after film growth. The initial substrate peak area ($A_{Si\ 2p,0}$) was not measured directly, since atmospheric contamination and its subsequent transformation in the reactor could not be excluded. Rather than directly measuring $A_{Si\ 2p,0}$, we generated the MoS_2 thickness curve by choosing the initial Si 2p area such that the XPS estimate at n=25 coincided with the cross-

sectional HRTEM measurement obtained from the same surface. This amounts to a single-point calibration against the TEM measurement and effectively introduces a y-offset. Similar to the composition-dependent uncertainty in IMFP, discussed in the previous paragraph, the y-offset does not modify in any way the linear trend observed in Figure 4 and the growth rate that was subsequently calculated.

Compositional Analysis by XPS Depth Profiling

XPS depth profiling was used to remove carbonaceous material from the surface of a thick MoS_2 film. At short sputter times (≤1 min), we removed the top few nm of material in order to eliminate contributions to the overall film composition from atmospheric contamination. The film was ≈25 nm in thickness (assuming a linear growth rate), which ensured that all emitted photoelectrons originated from within the film, rather than the substrate. Such a depth profile from a film grown using n=200 is shown in Figure S5. Composition values were calculated using the peak areas for the O 1s, C 1s, Mo 3d, and S 2p regions. Nitrogen was not detected in these films. Relative sensitivity factors were provided by the instrument manufacturer (Kratos Analytical) and were used as given in the CasaXPS software package.

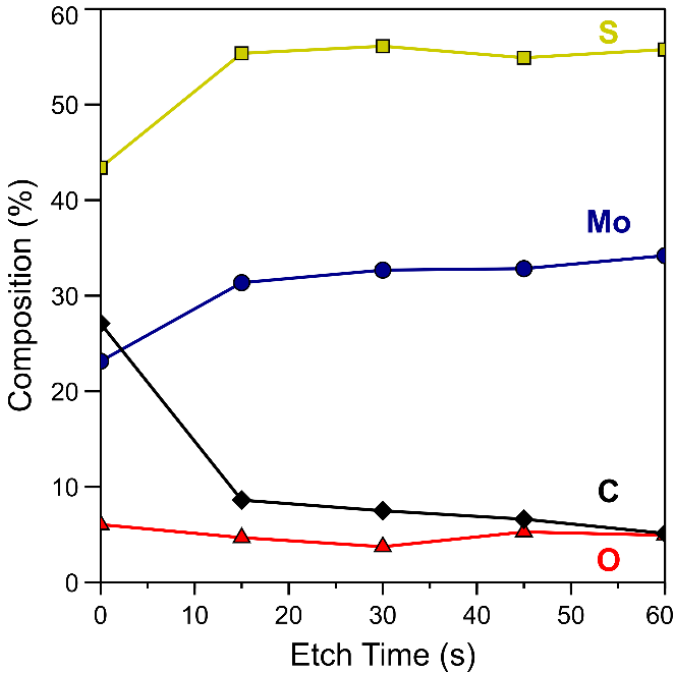

Figure S5. XPS depth profile of a thick MoS_2 specimen (n=200) using a 4 keV Ar^+ ion beam.

XPS Survey Scans for Films Grown with and without Et_2S_2

Survey scans from two sets of thick films growth with and without Et_2S_2 are shown in Figure S6. These complement the high resolution scans discussed in the main text and also shown in Figure 7. The notable feature in the survey scans is the presence of the N KLL transition for the film grown without Et_2S_2, which supports the interpretation of the Mo 3d region and the assignment of the N 1s feature.

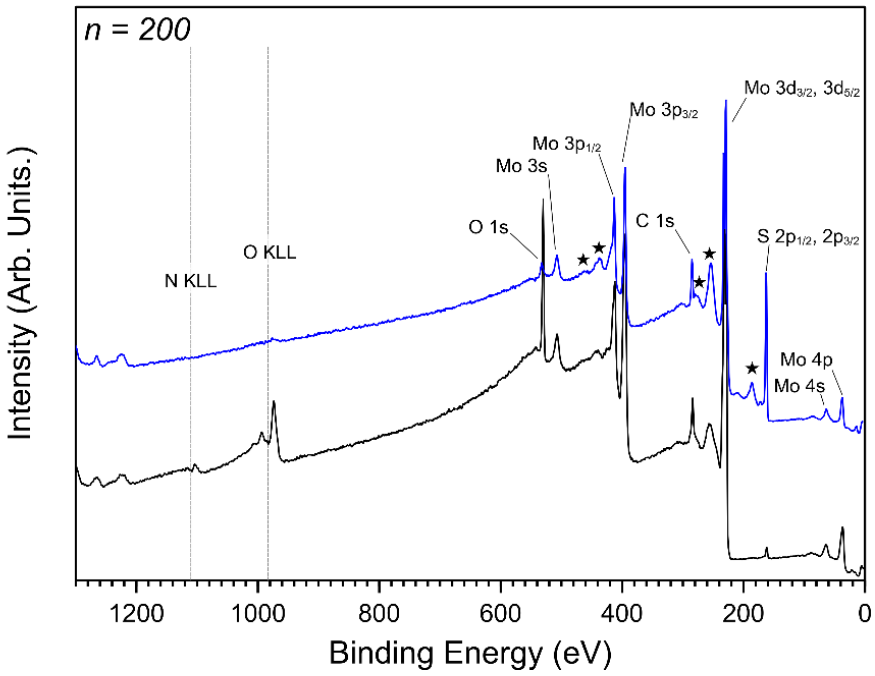

Figure S6. Survey scans from films grown using $(N^tBu)_2(NMe_2)_2Mo$ only (black trace) and those grown using the Mo source and Et_2S_2 (blue trace). Positions of the N and O Auger transitions are marked with dashed lines. Features identified with a star (★) are generally associated with MoS_2, including plasmon peaks.

Wafer-Scale Uniformity

To investigate film uniformity on 50 mm diameter substrates, one of the fused quartz wafers shown in Figure 2 in the main text was measured using XPS. Spectra from the Si 2p core level region were recorded for 8 distinct points at 5 mm intervals along the centerline of the wafer. The edges of the wafer were omitted to exclude signal from the sample clips. Film thickness was calculated using Si 2p attenuation as described above, assuming an MoS_2 overlayer. An uncoated quartz wafer was used as a reference. For a film grown using 15 injections (n = 15), coating thickness was estimated at 3.9 nm with a standard deviation of 0.1 nm for the ≈ 35 mm long region sampled. Note that film thickness on fused quartz is larger than

on thermal SiO_2/Si, which could be explained by differences between the two substrates. While the thermally oxidized Si wafers are expected to have smooth surfaces, the polished silica wafers we used for this demonstration are not semiconductor grade substrates and therefore do not have roughness specifications. Since the XPS measurement does not account for morphology, attenuation of the substrate signal and the calculated film thickness will depend on roughness. Surface temperatures during growth are also likely to be different due to emissivity differences between the two substrates.

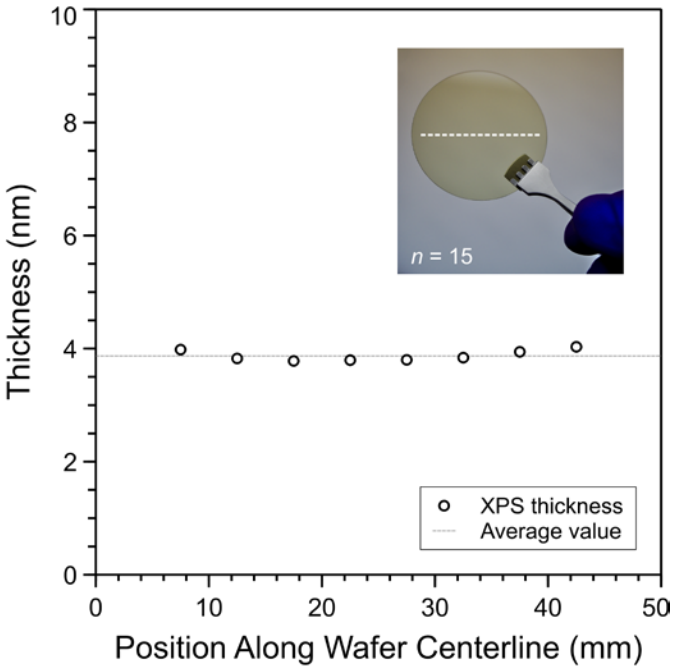

Figure S7. Thickness profile from a 50 mm fused quartz wafer coated using 15 injections (*n* = 15) of $(N^tBu)_2(NMe_2)_2Mo$ and Et_2S_2 at nominally 591 °C. Film thickness values are calculated by XPS. The dashed line in the inset denotes the approximate region from which individual spots were measured.

XPS Data Processing and Peak Fitting

High resolution XPS data were modeled using synthetic peak shapes as provided by the CasaXPS v2.3.17 software package. Line shapes defined as GL were a mixture of Gaussian and Lorentzian components. Those termed as A denote a modified Voigt function. Those termed as LA denote an asymmetric Lorentzian function. Background types were Shirley or linear, depending on the region. Binding energy correction was done based on the S $2p_{3/2}$ peak (S-Mo, 226.3 eV[3]) assigned to MoS_2. We used S 2p because the composition of the C 1s region changed based on the deposition chemistry, *i.e.* growths done with and without Et_2S_2 showed distinct changes in the carbon spectra and the C-H peak typically used for charge calibration could not be reliably identified. Conveniently, S $2p_{3/2}$ could be used as a stable reference point for all measurements because residual sulfur in the reactor produced a small amount of MoS_2 even in the growth runs conducted without Et_2S_2 injections.

Table S2. Peak assignments, positions, shapes, and fitting constraints used in the XPS analyses for films grown with and without Et_2S_2.

Transition	Position (eV)	Assignment	Peak Shape	Constraints
Mo 3p	417.4	Plasmon	GL(30)	None
Mo $3p_{3/2}$	399.0	MoO_3	GL(50)	None
Mo $3p_{1/2}$	416.5	MoO_3	GL(50)	Area, position
Mo $3p_{3/2}$	395.0	MoS_2	GL(50)	None
Mo $3p_{1/2}$	412.5	MoS_2	GL(50)	Area, position
N 1s	397.8	Mo_xN_y	GL(90)	None
C 1s	284.2	Graphitic carbon	A(0.29,0.61,0)GL(0)	None
C 1s	284.5	C-H	GL(30)	FWHM
C 1s	286.6	C-O	GL(30)	FWHM
C 1s	288.6	C=O or C-N	GL(30)	FWHM
Mo $3d_{5/2}$	229.1	MoS_2	LA(2.9,4,6)	None
Mo $3d_{3/2}$	232.3	MoS_2	LA(2.9,4,6)	Area
Mo $3d_{5/2}$	232.5	MoO_3	GL(50)	FWHM, position
Mo $3d_{3/2}$	235.6	MoO_3	GL(50)	None
Mo $3d_{5/2}$	228.9	Mo_xN_y	LA(1.35,5,6)	None

Mo $3d_{3/2}$	232.1	Mo_xN_y	LA(1.35,5,6)	Area
S 2s	226.4	MoS_2	GL(90)	None
S $2p_{3/2}$	162.0	MoS_2	GL(50)	None
S $2p_{1/2}$	163.2	MoS_2	GL(50)	Area
Si 2s	154.4	SiO_2	GL(30)	None
Si 2p	103.7	SiO_2	GL(30)	None

REFERENCES

(1) Powell, C. J.; Jablonski, A. *J. Phys. Chem. Ref. Data* **1999**, *28* (1), 19–62.

(2) Mitchell, D. F.; Clark, K. B.; Bardwell, J. A.; Lennard, W. N.; Massoumi, G. R.; Mitchell, I. V. *Surf. Interface Anal.* **1994**, *21* (1), 44–50.

(3) Ganta, D.; Sinha, S.; Haasch, R. T. *Surf. Sci. Spectra* **2014**, *21* (1), 19–27.